Detailed Structure of Skin[2]

The skin consists of various layers, as indicated in Figs. 2.5 and 3.16. An outer layer (the *epidermis*) overlays the inner dermis. The epidermis consists principally of keratin, derived from dead cells of the lower layers, arranged in a flattened and irregular fashion. The bonding strength of these cells is low. They are constantly flaking away naturally and can be easily broken or removed. The germinating layer at the boundary of the epidermis contains a mixture of living and dead cells. The dermis contains living cells and a great density of blood vessels that are related to both nutrition of the skin and its thermoregulation. The dermis consists of bundles of *collagen* fibrils oriented in all directions, giving it strength and elasticity. The distribution of skin thickness varies greatly for different body areas. The epidermis itself ranges from about 10 to more than 100μm. It is typically 10 times

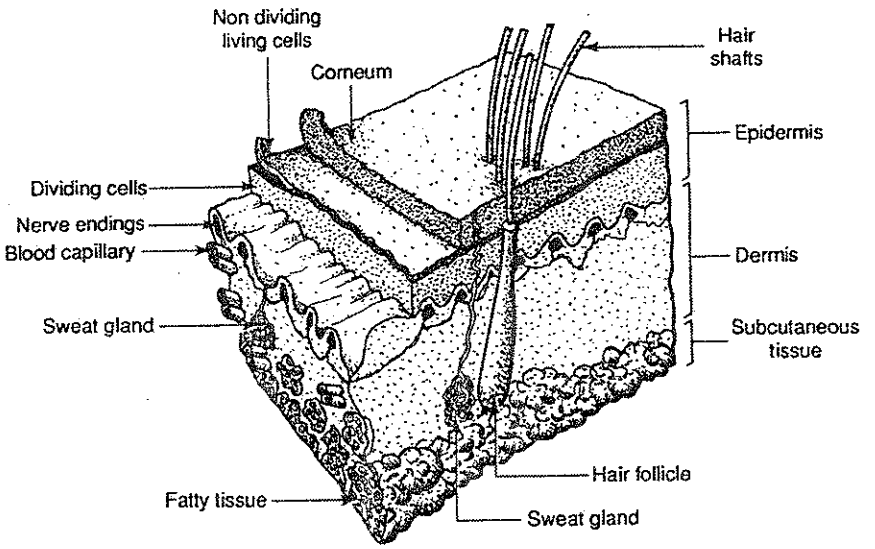

FIGURE 2.5. Structure of the skin.

[2]See also Edelberg (1971), Harkness (1971), and Tregear (1966).

as thick on the palms of the hands as compared with other body areas and is endowed with a much greater density of sweat glands.

The corneum (the outermost layer of dead skin cells) is a relatively poor conductor when dry. But when wet or sweaty, or when bypassed (as with an injury), the conductivity of the skin can rise dramatically. The contribution of the corneum to the total impedance can be studied by stripping the skin with cellophane tape (Harkness, 1971; Lykken, 1971; Tregear, 1966; Reilly et al., 1982; Clar et al., 1975). Figure 2.6 illustrates the drop of skin resistivity when the corneum is successively stripped away, showing an ultimate drop by a factor over 300. Impedance drop with corneal stripping has also been noted with high-voltage spark discharge stimuli (refer to Sect. 2.6). When a microelectrode penetrates the corneal layer, the resistance drops suddenly, as noted in Table 2.2 (Suchi, 1954).

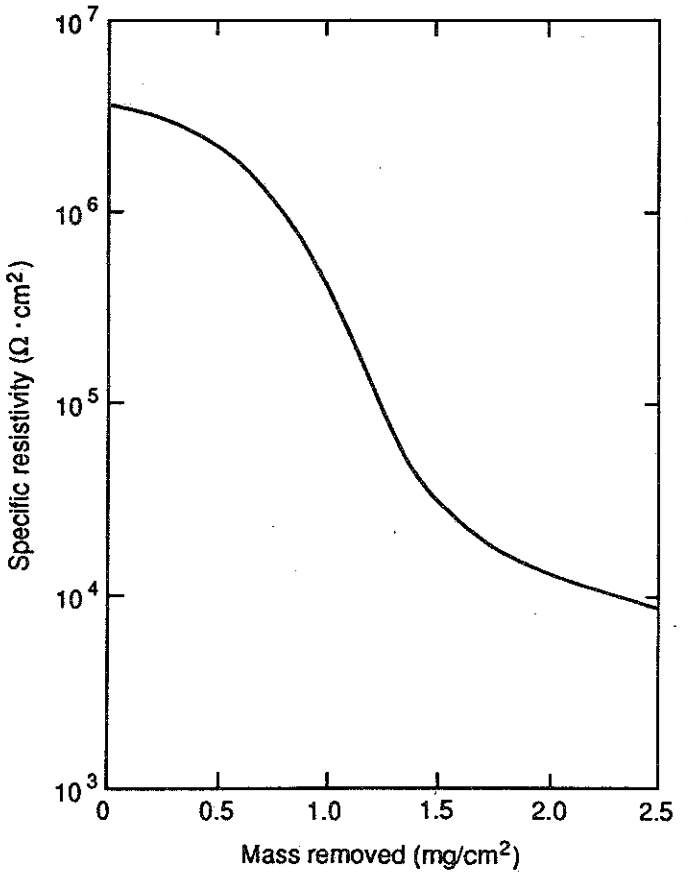

FIGURE 2.6. Impedance of skin as related to the mass of corneum removed from dry skin; sinusoidal current at 1.5 Hz. (Adapted from Tregear, 1966.)

TABLE 2.2. Impedance layers in the epidermis.

	Ball of thumb	Forearm
Dry, outer layer thickness (μm)	200	45
Penetration distance for impedance breakdown (μm)	350	50

Source: Suchi (1954).

Sweat is chiefly a 0.1 to 0.4% saline solution of sodium chloride, with a resistivity of 140 Ωcm at 37°C (for a 0.3% solution). The density of sweat ducts (per cm^2) is approximately 370 on the palmar and plantar surfaces of the hands and feet, 160 on the forearm, 750 at the bend of the elbow, 150 to 250 on the breast, and 60 on the buttocks.

Current appears to be conducted in dry skin through discrete channels beneath a contact electrode. With a multipoint electrode, current is found to be preferentially conducted at one point (Mueller et al., 1953). In experiments with electroplating on the skin surface (Saunders, 1974), the pattern of silver deposition on the arm shows that current is conducted in discrete channels at a density of about 1 channel/mm^2. Other electroplating experiments reveal that the channel density on the palm is about three times that on the forearm (Panescu et al., 1993). These observations approximately correspond to the density and distribution of sweat ducts on the hand and forearm. The punctate nature of skin conductance was also explored with high-voltage discharges (Sect. 2.6).

The sweat ducts form electrical weak points in the epidermis, acting as conductive tubes into the well-conducting dermis and tissues below. Suchi (1954) explored the impedance role of sweat ducts using a silver microelectrode to scan various parts of the skin. When the electrode touched a duct filled with sweat, the impedance dropped by a factor of 10 as compared with adjacent areas of the skin. If the duct was dry, the drop was approximately a factor of two.

Equivalent Circuit Models

It would be desirable to represent the impedance of the skin and body as an equivalent circuit model that allows one to determine internal currents for a wide range of exposure conditions. Unfortunately, the skin is not readily expressible as a simple passive circuit—it is a distributed electrical system having markedly nonlinear and time-variant properties complicated by electrolytic interactions at the electrode interface. Nevertheless, impedance models are often valid under a sufficient range of circumstances to be of practical use.

A simple model sometimes used to represent skin impedance is a parallel network consisting of a capacitor and resistor, followed by a series resistor

(cf. Yamamoto and Yamamoto, 1977; Burton et al., 1974). The parallel resistor and capacitor represent the resistivity and capacity of the skin, and the series resistance the well-conducting subepidermal medium. Evidence for this simple model can be seen when measuring the current response to a constant-voltage stimulus pulse applied to the skin as illustrated in Fig. 2.7 (from Lykken, 1971). The response, illustrated in Fig. 2.7b, shows an initial current spike that is limited by the series resistance, R_s. Afterward, the current decays to the value limited by $R_p + R_s$. After the corneum has been removed by abrading, the current, illustrated in Fig. 2.7c, is limited by R_s.

A more complete model considers the skin as composed of numerous layers of cells, each having capacitance and conductance, as illustrated in Fig. 2.8a (Edelberg, 1971; Lykken, 1971). The individual strings of elements are meant to represent the parallel paths beneath an electrode. In addition to the resistance and capacitance elements, the electrical model contains DC potential sources to account for the observed bulk potential of the skin of about 15 to 60 mV, with the surface negative relative to the underlying layers. These potentials are extremely small in comparison with the stimulus potentials typically needed for cutaneous electrical stimulation. The element R_B is treated as the body impedance, exclusive of the skin.

Figure 2.8b illustrates a model of intermediate complexity. The element Z_e represents the impedance at the electrode interface; it is seldom determined explicitly, but rather is lumped together into total impedance. The parallel RC circuit represents the epidermis, with the element R_{P2} added in the capacitive branch. It is shown in parentheses to indicate that it is

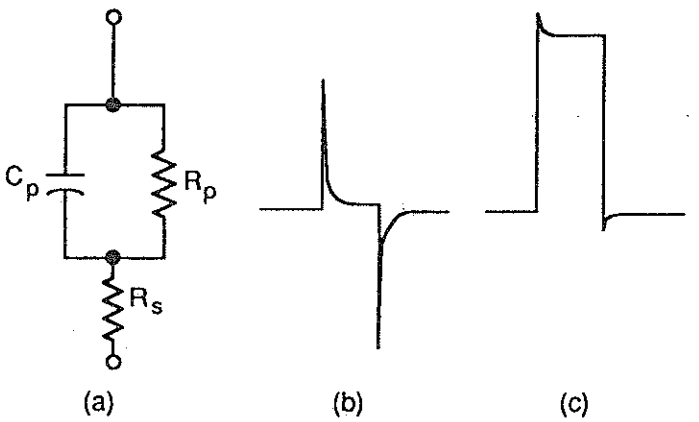

FIGURE 2.7. Current response of skin to square-wave constant-voltage pulses: (a) equivalent circuit; (b) response of intact skin; (c) response of skin with corneum removed. (Copyright 1971, The Society for Psychophysiological Research. Reprinted with permission of the publisher and the author from Lykken, 1971.)

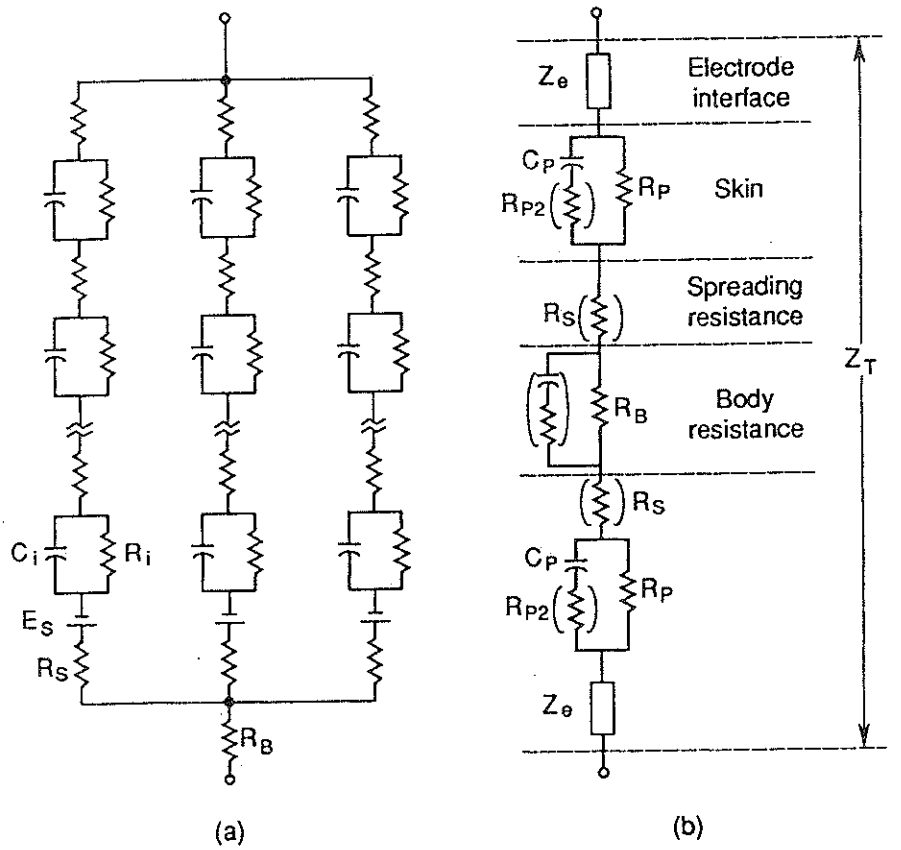

FIGURE 2.8. More complex impedance models: (a) multilayer model for skin impedance; (b) simplified body impedance model.

frequently ignored in impedance representations. The subepidermal layer is shown as consisting of a spreading resistance element, R_s, which is inversely related to electrode size, and a body resistance element, R_B, which increases with electrode separation. In most studies of body impedance, R_s and R_B are lumped together into a single resistive term. The element R_B is generally treated as a pure resistance, although in fact it contains a small reactive component, indicated by the components in parentheses. The reactive component can be ignored for most practical applications. The circuit representation includes additional terms to account for the second electrode. The total circuit impedance is designated Z_T. The circuit models discussed here are merely approximations that are sometimes suitable; the individual terms may behave in a more complex fashion than would a laboratory component, as discussed below.

Area Proportionality of Skin Admittance

From geometric considerations, it might seem reasonable to suppose that skin admittance is directly proportional to contact area, as long as the electrode diameter is significantly larger than the skin thickness. Many investigators report equivalent circuit parameters as being area proportional. Lykken (1971), for example, notes an area-proportional admittance for DC currents with electrodes of $0.72\,cm^2$ and larger and for pulse stimuli with electrodes $2.4\,cm^2$ and larger. Tregear (1966) reports that the product of impedance and area is constant for wet skin only for electrodes having areas larger than $2\,cm^2$. For smaller areas, the impedance departs considerably from inverse area proportionality, with significant differences between wet and dry skin. Biegelmeier and Rotter (1971) evaluate equivalent circuit parameters for electrodes of 1.5 and $100\,cm^2$ (an area difference of 67:1); they note a 4:1 change in $R_{P2} + R_s$ as defined in Fig. 2.8b, and a 25:1 change in R_P, showing that admittance rises more slowly than does contact area.

The area-dependent portion of the resistive path (R_s in Fig. 2.8b) comprises the region where the current still undergoes spherical spreading from the stimulating electrode. At the point where current no longer spreads out with distance, the resistance is no longer dependent on electrode area, but is more a function of electrode separation and body geometry. Thus, R_B in Fig. 2.8b is taken to be independent of electrode contact area.

Area-proportional parameters are usually determined by dividing admittance by electrode contact area. This simple calculation is confounded by the fact that the distribution of current beneath a contact electrode may be very nonuniform, as demonstrated in theoretical (Caruso et al., 1979; Rattay, 1988) and experimental (Lane and Zebo, 1967) studies. Figure 2.9 illustrates the theoretical current density for a three-layer conductivity model representing a layer of skin, fat, and muscle tissue; a two-layer model consisting of fat and muscle; and a single-layer model consisting of muscle tissue (Caruso et al., 1979). For the three-layer model, the calculated current density near the electrode edge is nearly a factor of 10 greater than that at the center. For the single-layer model, the current density from center to edge differs by a factor of about 2.2. Area conductivity is further complicated by the fact that current travels laterally beyond the confines of the electrode, such that the effective contact area may be larger than the physical contact area. Rather than rely on area-proportional values, contact impedance at high-currents can be expressed more accurately in terms of both the area and perimeter of the contact, as given by Equation 10.5.

With these caveats in mind, Table 2.3 lists some of the area-proportional values reported for low-frequency (0- to 65-Hz) skin impedance (Tregear, 1966). Because of the low frequency, the list applies primarily to the resistive component $R_P + R_S$ defined in Figs. 2.7a and 2.8b. The values are a

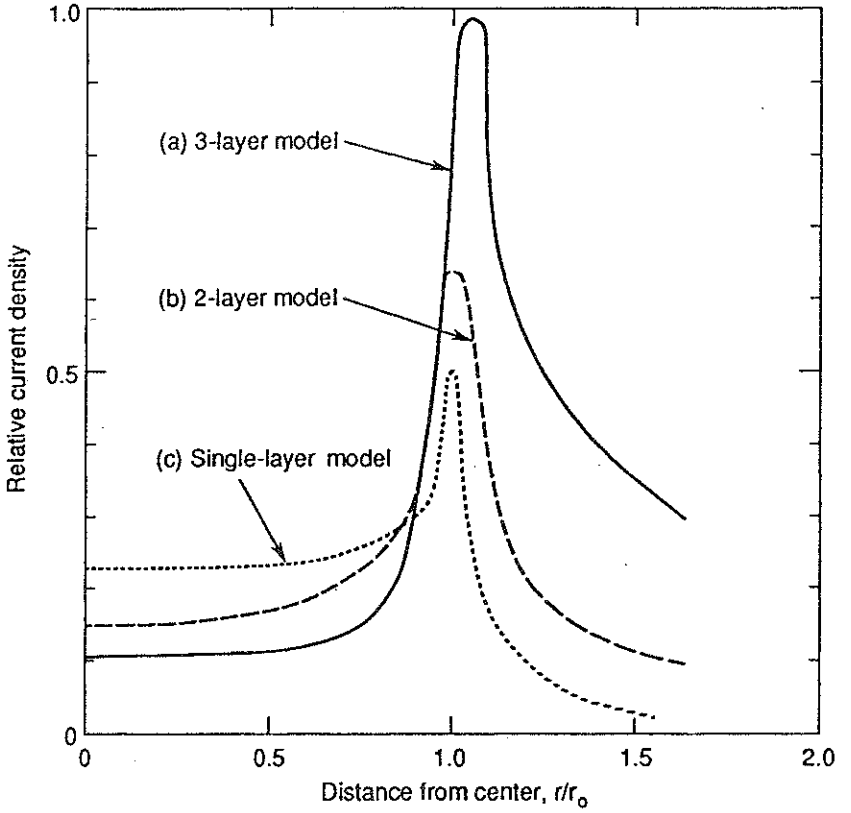

FIGURE 2.9. Current density beneath contact electrode; r_0 = electrode radius; vertical axis on dimensionless scale. (a) three layer model with skin, fat, and muscle; (b) two layer with fat and muscle; (c) single layer with muscle. (From Caruso et al., 1979.)

TABLE 2.3. Low-frequency resistivity of human and animal skin.

Species	Hydration	Body Location	Frequency (Hz)	Impedance ($k\Omega\,cm^2$)
Human	Dry	Arm	0	100–1,000
Human	Dry	Arm	1.5–10	600–1,200
Human	Dry	Fingertip	0–1	120–130
Human	Dry	Palm	30–65	60–80
Human	Wet	Forearm	1.5	880
Pig	Wet	Flank	1.5	12
Rabbit	Wet	Flank	1.5	18

Source: Adapted from Tregear (1966); data compiled from a variety of sources.

compilation from a variety of sources and do not necessarily represent data measured in a consistent manner.

Skin Capacitance

A variety of testing methods indicate that the skin's capacity lies in the range 0.02 to 0.06μF/cm^2 (Edelberg, 1971); by conventional calculations, this is considered very high. Consider, for example, a corneum thickness of 10μm and a dielectric constant of 2.5 for biological membranes. With these values, the capacity is calculated to be about $2 \times 10^{-4}\mu$F/cm^2—a small fraction of the experimental values.

Skin capacitance will be affected by *polarization capacitance*—the phenomenon of stored charges that appear around an electrode in an electrolytic medium, forming an effective ionic capacitor that is dependent on excitation frequency (Schwan, 1966). Lykken (1971) argued that the apparent frequency-dependent property of skin capacitance is simply a consequence of the choice of equivalent circuit and that a representation with a resistively coupled capacitor (C_P and R_{P2} in Figure 2.8b) will demonstrate a fixed value versus frequency.

Much of the skin's capacity lies in the corneum. If the corneum is stripped away, the skin capacitance is reduced with each successive stripping operation (Edelberg, 1971). When the corneum is removed entirely, the capacity drops to a small fraction of its intact value (Lykken, 1971; vanBoxtel, 1977). These observations are counter to a model in which the corneum is simply a dielectric separating the electrode and the underlying conductive dermis. If that model were correct, we would expect to see an increase of capacitance as the thickness of the corneum is reduced. Biegelmeier and Miksch (1980) postulate that the skin's capacity is derived from membrane capacitance of the sweat gland duct. However, this explanation does not account for the leading-edge current spikes that are observed when constant-voltage pulses are applied to the sweat-gland-free skin of Rhesus monkeys (Bridges, 1985).

An alternative explanation for the skin's high capacity was provided by Tregear (1966), who treated the skin capacitance as being due to individual cell membranes as in Fig. 2.8a. If we assume that each cell's membrane may have a capacity as large as 5μF/cm^2, and acknowledging that each cell accounts for two membrane layers, then 200 cell layers could account for a capacitance of 0.05μF/cm^2. A related mechanism that might account for skin capacitance has been described as an ionic bilayer surrounding individual corneal cells (Clar et al., 1975).

Time-Variant and Nonlinear Aspects of Skin Impedance

When an electrode is placed on dry skin, impedance gradually falls with time, as noted in Fig. 2.10 (Mason and Mackay, 1976). During the first 2 min,

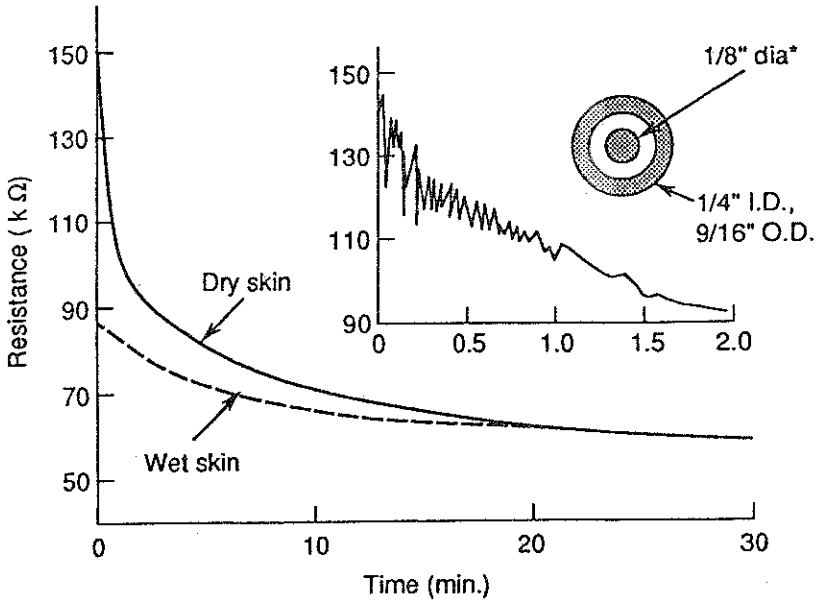

FIGURE 2.10. Variation of skin resistance with time. Concentric electrode as illustrated (inner diameter not clearly described in source). Wet skin treated with tap water. Inset shows expanded scale for first 2 min. Stimulus current: 1 mA. (Adapted from Mason and Mackay, 1976, ©1976 IEEE.)

the impedance undergoes rapid fluctuations superimposed on a relatively sharp overall drop (see insert). Thereafter, the impedance continues to drop, reaching an apparent asymptotic value after some 20 or 30 min. This effect may be explained by gradual hydration of the corneum from sweat buildup beneath the electrode. In the same experiments, skin pretreated with conductive electrode paste started with an initially lower impedance, rose somewhat, and attained a final value only slightly below its initial value after about 1 min.

Past studies have shown that the electrical properties of the skin are nonlinear. Edelberg (1971) suggests that the linear region for current density lies in the range below 2 mA/cm^2. Lykken (1971) concludes that it is applied voltage, and not current density, that determines an upper limit of linearity around 2V. Biegelmeier and Rotter (1971) note variations in equivalent circuit values of over 2:1 for voltage changes from 4 to 45 V. Stevens (1963) defines the DC current conducted in dry skin in terms of $I = aV + bV^2$, in which the V^2 term dominates above 3V.

Nonlinear phenomena in living skin was studied by Grimnes (1983a). He hypothesized that the time scale of impedance changes could be explained by either a nondielectric mechanism or a dielectric breakdown mechanism,

depending on the applied voltage in the range of 600 to 1,000 V. In this work, the current was limited to a few microamperes, and the results may not necessarily apply directly to higher current densities.

A dramatic display of skin nonlinearity is seen in the sudden break-down of impedance above a critical voltage. Dielectric breakdown of dry, excised corneum has been observed by Mason and Mackay (1976) at 600V for a 15-μm-thick sample and at 450 V by Yamamoto et al. (1986). Dielectric breakdown of intact skin from high-voltage spark discharges appears at similar voltages, as described in Sect. 2.6.

With intact, living skin, a sudden impedance breakdown has been observed at significantly lower voltages than that needed to break down excised corneum. A discrete thermal model has been developed to account for nonlinear skin impedance, including breakdown (Panescu et al., 1994a,b). Pricking pain has been associated with the impedance breakdown (Nute, 1985; Gibson, 1968; Mason and Mackay, 1976; Mueller et al., 1953). During breakdown, current becomes concentrated in discrete channels. According to Mason and Mackay, microscopic examination of the electrode site reveals small blackened punctures under a dry-skin electrode, but no such evidence when the skin has been pretreated with water or electrode paste.

The major source of skin nonlinearity lies in the corneum. Equivalent circuit values R_P and R_S were evaluated by van Boxtel (1977) from the transient current response to constant-voltage pulses. With intact skin, R_P varied significantly with the applied voltage, whereas R_S remained independent of the stimulus level (up to a voltage of 40 V, and 40 mA final current). With the corneum removed, both R_P and R_S remained independent of the stimulus level.

Figure 2.11 illustrates nonlinear impedance response for pulses of 5-μs duration (Saunders, 1974). At these short durations, the corneal layer is probably bypassed through capacitive coupling to the dermis. However, the skin exhibits marked nonlinear properties, as noted in the knee of the curves at the higher current and voltage values—nonlinear breakdown occurs with voltages from about 150 to 250 V.

Freiberger (1934) describes breakdown as occurring at small contact areas within a fraction of a second for voltages above 100 V. Biegelmeier and Miksch (1980) noted breakdown above 200V for large hand-held electrodes (refer to Sect. 2.3). With small electrodes and voltages above 100 V, breakdown may occur within fractions of a second with dry-skin contact.

Nonlinear response to sinusoidal voltage shows up as distortions from a sinusoidal current waveform. Short-term distortions appear as an instantaneous nonlinear response within individual cycles; longer term nonlinearities appear as a gradual reduction of impedance. Figure 2.12 illustrates impedance breakdown with 50-Hz AC stimulation on a relatively long time scale (Freiberger, 1934). An initial precipitous drop occurs within

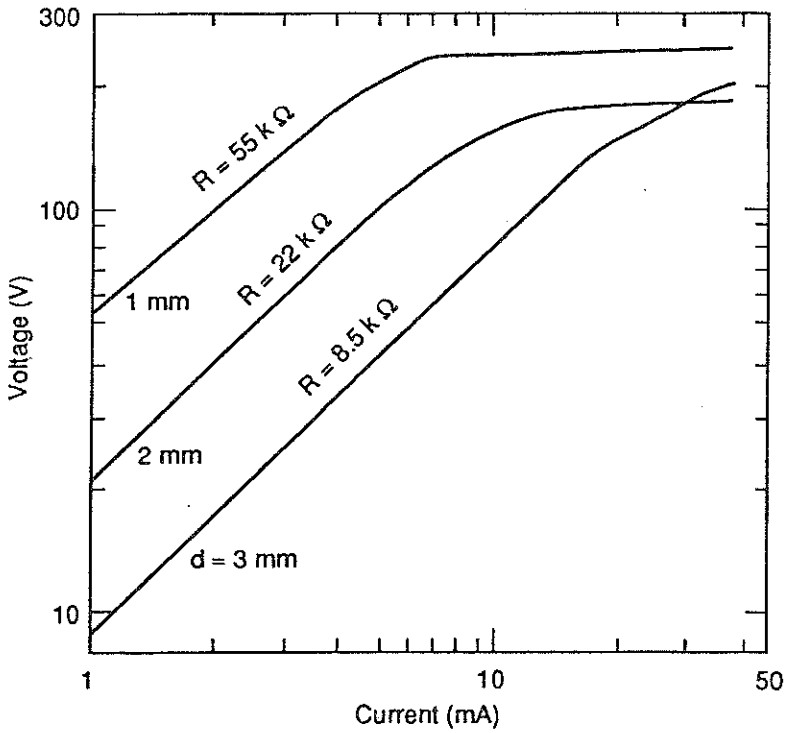

FIGURE 2.11. Nonlinear voltage/current relationship for 5-μs cathodic pulses applied to abdomen; resistance (R) applies to linear regions of curves; d = electrode diameter. (Adapted from F.A. Saunders, 1974 in *Conference on Cutaneous Communication Systems and Devices*, pp. 20–26, reprinted by permission of Psychonomic Society, Inc.)

a small fraction of a minute, a second drop during the first minute, and a final gradual drop during the next 7 or 8 min.